SUPPLEMENTARY DATA

The Increasing Surface Ozone and Tropospheric Ozone in Antarctica and Their Possible Drivers

Pankaj Kumar[1], Jayanarayanan Kuttippurath[1,*], Peter von der Gathen[2], Irina Petropavlovskikh[3,4], Bryan Johnson[4], Audra McClure-Begley[3,4], Paolo Cristofanelli[5], Paolo Bonasoni[5], Maria Elena Barlasina[6], and Ricardo Sánchez[6]

[1] CORAL, Indian Institute of Technology Kharagpur, Kharagpur 721302, India
[2]Alfred Wegener Institute, Helmholtz Centre for Polar and Marine Research, Telegraphenberg A45-N, Potsdam 14473, Germany
[3] Cooperative Institute for Research in Environmental Sciences, University of Colorado, Boulder, Colorado 80309, USA

[4] NOAA, ESRL Global Monitoring Laboratory, Boulder, Colorado 80305-3328, USA

[5] National Research Council of Italy, Institute of Atmospheric Sciences and Climate, Bologna 40129, Italy

[6] Servicio Meteorológico Nacional, Vigilancia de la Atmosfera y Geofísica, Av. Dorrego 4019, Buenos Aires, Argentina

*Corresponding author: Dr. Jayanarayanan Kuttippurath
CORAL, IIT Kharagpur
Kharagpur-721302, India
Phone: +91 3222 281994
E-mail: jayan@coral.iitkgp.ac.in

Number of pages: 20

Number of tables: 4

Number of figures: 12

METHODS

Ozone profile Aggregation

As ozone measurements from coastal and inland stations are expected to have very distinct characteristics, we employ the weighted mean of available measurements and corresponding reduced chi-square corrected standard error for trend analysis.

Here, Weight for station j is:

$$weight_j = \frac{1}{\sigma_j^2 * n_j} \tag{1}$$

Normalized weight is estimated as follows:

$$w_j = \frac{weight_j}{\sum_{j=1}^{n} weight_j} \tag{2}$$

Weighted mean for a particular month is calculated as:

$$\acute{y} = \sum_{j=1}^{n} w_j y_j \tag{3}$$

Standard error of weighted mean is calculated using:

$$\sigma_{\acute{y}}^2 = \sum_{j=1}^{n} w_j^2 \sigma_j^2 \tag{4}$$

Reduced chi-square corrected standard error is calculated using:

$$\hat{\sigma}_{\acute{y}}^2 = \sigma_{\acute{y}}^2 \chi^2 \tag{5}$$

where reduced chi-square is given as:

$$\chi^2 = \frac{1}{n-1} \frac{\sum_{j=1}^{n} \left(y_j - \acute{y} \right)^2}{\sigma_j} \tag{6}$$

where y_j and σ_j is monthly mean and standard deviation for station j, and n_j is number of stations of the same kind (coastal/inland) and n is the total number of stations considered in this study.

Dynamic Linear Model (DLM)

To specifically attribute the factors responsible for ozone variability, both the Multiple Linear Regression (MLR) (discussed in the main text) and the Bayesian Dynamic Linear Model (DLM)[1–4] are used.

In DLM, we model time-series observations y_t at time t as follows:

$$y_t = F_t x_t + v_t, v_t \sim N(0, V_t) \quad (7)$$

$$x_t = G_t x_{t-1} + w_t, w_t \sim N(0, W_t) \quad (8)$$

where x_t is the *unobserved state* containing the (non-linear) trend, the seasonal cycle, dynamical coefficients of the regressor variables, and the auto-regressive (AR) process.

$$x_t = \left(x_t^{trend}, x_t^{seas}, x_t^{regressors}, x_t^{AR}\right) \quad (9)$$

The *state evolution operator* G_t and the *model error covariance* W_t govern the stochastic evolution of the state whereas the *observation matrix* F_t projects it onto the observations.

Here, trend X_t^{trend} is modeled as a random walk process which is, in turn, defined by two states: local background level μ_t and local trend α_t.

$$x_t^{trend} = (\mu_t, \alpha_t) \quad (10)$$

$$\mu_t = \mu_{t-1} + \alpha_{t-1} \quad (11)$$

and

$$\alpha_t = \alpha_{t-1} + \epsilon_{trend}, \epsilon_{trend} \sim N(0, \sigma_t) \quad (12)$$

The non-linearity of the background trend, is governed entirely by the parameter σ_{trend}. σ_{trend} is a free parameter to be fit simultaneously with the rest of the regression model.

Thus, DLM is distinct from MLR in the sense that the trend is not predetermined, but it is free to vary smoothly over time, and the degree of trend variability (σ_{trend})is a parameter that is estimated a-posteriori from the data using Markov chain Monte Carlo (MCMC) sampling using data driven prior for trend variability. DLM can easily capture change in trend for which various studies used independent-linear trends or piecewise linear regression, and does not require a-priori determination of turnaround time. In comparison to the MLR, which is based on the premise that the error distribution on measurements is constant in time (homoscedasticity), DLM implements heteroscedastic time-varying uncerainties. Moreover, DLM also allows the amplitude of the seasonal cycle to vary dynamically with time. Please see Laine et al. 2014[1] for detailed discussions about DLM.

In our study, the state is constituted by the (non-linear) trend, seasonal cycle with two components (with 6- and 12-month periods respectively), a number of regressor variables (represented by proxies) and an AR1 process. DLM trends has been calculated only for monthly mean data. A python library DLMMC has been used for performing the DLM analysis[5].

TABLES

Table S1: Antarctic stations with surface ozone measurements. Here latitudes and longitudes are in degrees; whereas altitudes are in meters from the mean sea level (agl).

Stations	Latitude (°N)	Longitude (°E)	Altitude (m)	Period
Arrival Heights	-77.83	166.67	184	1997–2018
Concordia	-75.09	123.33	3233	2006–2013
Neumayer	-70.65	-8.25	42	1993–2018
South Pole	-89.98	-24.80	2810	1993–2018
Syowa	-69.00	39.58	16	1997–2014

Table S2: Surface ozone and tropospheric ozone column (TOC) trends along with its standard error (in parenthesis) calculated using SLR and MLR. The trends are estimated in accordance with the availability of data at each station. The Arrival Heights surface ozone measurements are for the period 1997–2018, Concordia 2006–2013, Syowa 1997-2014, Neumayer 1993– 2018, and South Pole 1993–2018. Trend values are in ppbv yr $^{-1}$ for surface ozone and in DU yr^{-1} for TOC.

Sampling	Arrival Heights	Concordia	Neumayer	South Pole	Syowa	TOC
			SLR			
Monthly	0.134 (0.067)	-0.208 (0.204)	0.084 (0.048)	0.161 (0.036)	0.109 (0.079)	0.005 (0.019)
Annual	0.121 (0.047)	-0.362 (0.101)	0.077 (0.022)	0.146 (0.030)	0.091 (0.039)	-0.000 (0.007)
DJF	0.146 (0.060)	-0.625 (0.335)	0.031 (0.032)	0.111 (0.047)	-0.005 (0.055)	0.004 (0.011)
MAM	0.145 (0.056)	-0.360 (0.122)	0.137 (0.024)	0.226 (0.035)	0.105 (0.048)	0.031 (0.006)
JJA	0.140 (0.047)	-0.224 (0.060)	0.079 (0.035)	0.170 (0.032)	0.158 (0.058)	-0.024 (0.013)
SON	0.067 (0.053)	-0.088 (0.160)	0.058 (0.034)	0.077 (0.032)	0.092 (0.056)	-0.013 (0.016)
			MLR			
Monthly	0.115 (0.040)	-0.436 (0.138)	0.083 (0.019)	0.133 (0.025)	0.109 (0.031)	-0.002 (0.007)
Annual	0.098 (0.069)		0.098 (0.043)	0.002 (0.091)	0.092 (0.061)	-0.006 (0.010)
DJF	0.089 (0.106)		0.022 (0.031)	-0.096 (0.196)	-0.046 (0.068)	0.001 (0.014)
MAM	0.151 (0.110)		0.093 (0.033)	0.023 (0.094)	0.236 (0.087)	0.025 (0.008)
JJA	0.190 (0.081)		0.087 (0.050)	0.231 (0.062)	0.082 (0.081)	0.000 (0.015)
SON	0.094 (0.063)		-0.018 (0.066)	0.102 (0.062)	0.124 (0.088)	-0.033 (0.028)

Table S3: Contribution of proxies to surface ozone and tropospheric ozone column (TOC) variability at different stations. Here, solar flux (SF) represent the influence of solar activity, heat flux (HF) represent the residual circulation, potential vorticity (PV) accounts for the influence of polar vortex and stratosphere-troposphere exchange, and aerosol optical depth (AOD) accounts for aerosol loading and volcanic eruptions. AAO represents the Antarctic oscillation, multivariate ENSO index (MEI) represents the ENSO impact, and QBO represents the meteorological changes in the tropics by the Quasi-biennial oscillation. All values are in percentage [%].

Proxies	Arrival Heights	Concordia	Neumayer	Syowa	South Pole	TOC
AAO	9.0976	5.0805	1.5210	6.228	7.617	20.980
AOD	0.5830	0.4650	2.0440	1.365	5.555	3.822
HF	77.7617	58.3716	72.9089	77.794	36.096	12.415
MEI	6.5299	4.2544	3.9638	1.801	4.717	4.810
PV	0.3106	1.5484	3.8222	2.361	8.283	11.257
QBO	2.5774	14.0453	7.6927	4.640	11.372	17.947
SOLAR	0.5623	2.1894	0.3546	1.171	14.988	10.823

Table S4: Variable influence factor (VIF) for external forcings included in surface ozone analyses at Syowa.

FORCING	VIF
SOLAR FLUX	1.061
QBO_{30}	2.030
QBO_{50}	2.253
MEI	1.205
AAO	1.138
HEAT FLUX	1.103
PV	2.441
AOD	1.184

FIGURES

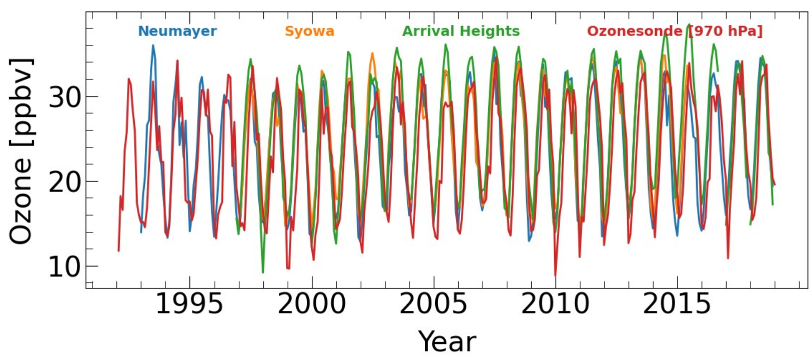

Figure S1: *Monthly time-series of surface ozone at different stations in Antarctica and weighted mean of ozonesonde based ozone observations at 970 hPa.*

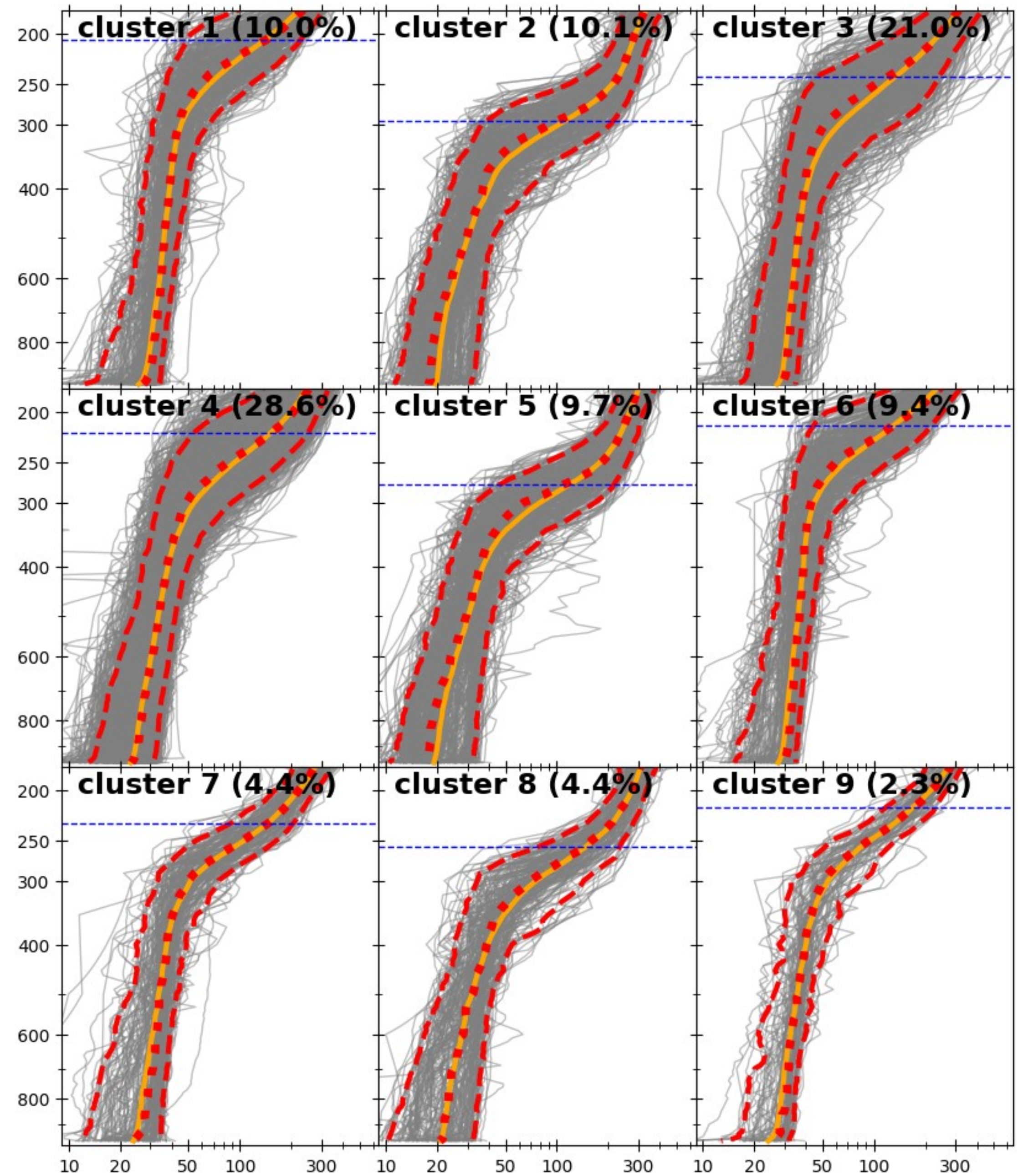

Figure S2: *The SOM-based 3x3 clusters of Antarctic ozone profiles. The orange solid lines depict the mean profiles of the cluster, red dotted lines represent median ozone profiles whereas 5th and 95th percentiles are shown in red dashed lines.*

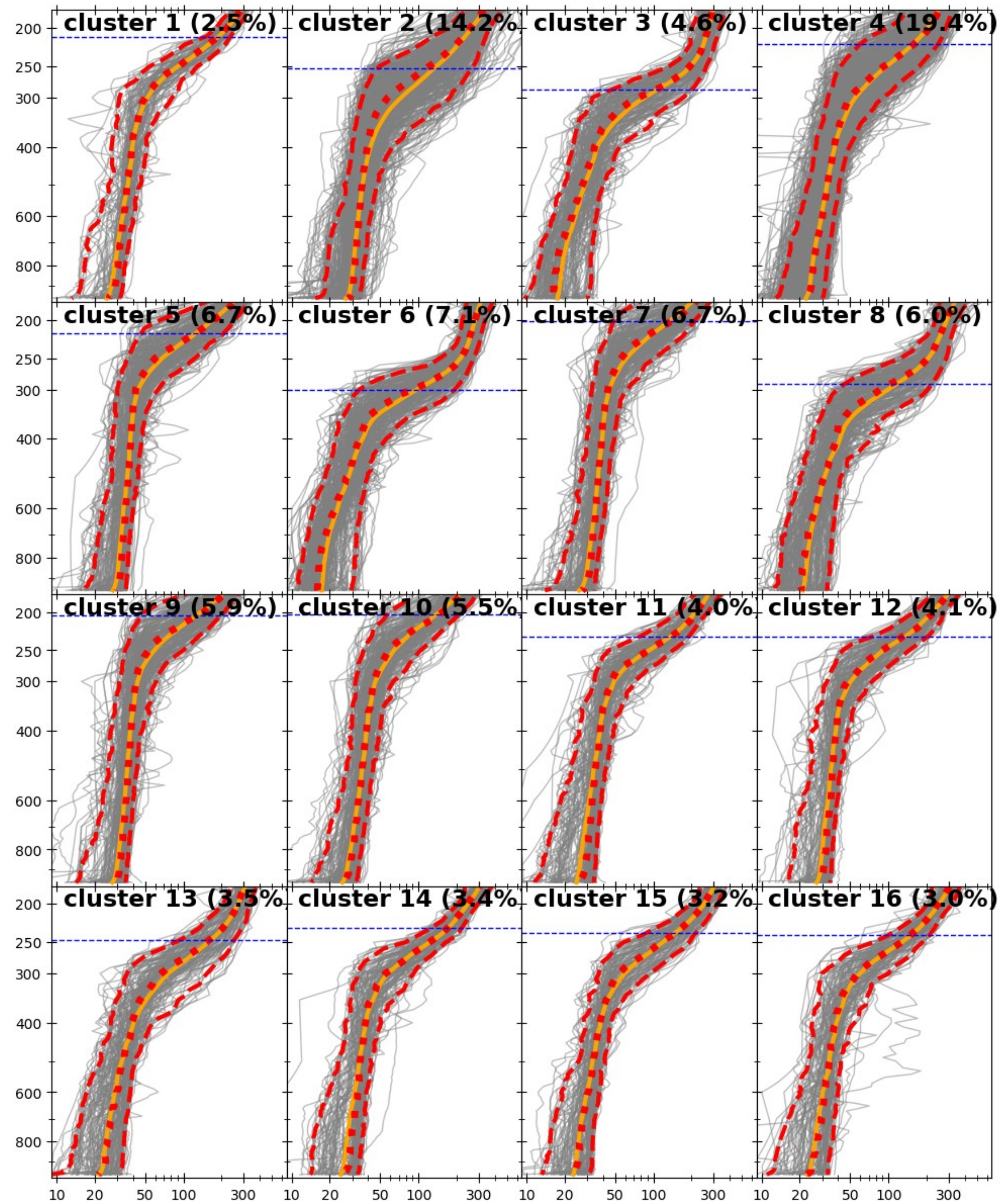

Figure S3: *The SOM-based 4x4 clusters of Antarctic ozone profiles. The orange solid lines depict the mean profiles of the cluster, red dotted lines represent median ozone profiles whereas 5th and 95th percentiles are shown in red dashed lines.*

Fig. S2 displays the 3x3 SOM nodes of Antarctic ozone profiles. Here, 3 clusters have less than 5 percent of the total number of profiles, while 5 clusters have less than 10 percent of the total number of profiles. Just 3 clusters have more than 10% ozone profiles.

Fig. S3 displays the 4x4 SOM nodes of Antarctic ozone profiles. Here, 8 clusters have less than 5 percent of the total number of profiles, while 14 clusters have less than 10 percent of the total number of profiles. Just 2 clusters have more than 10% ozone profiles.

Consequently, both Fig. S2 and Fig. S3 indicate that in most of their clusters, 3x3 and 4x4 SOM nodes comprise very few profiles and their geophysical interpretation is very difficult.

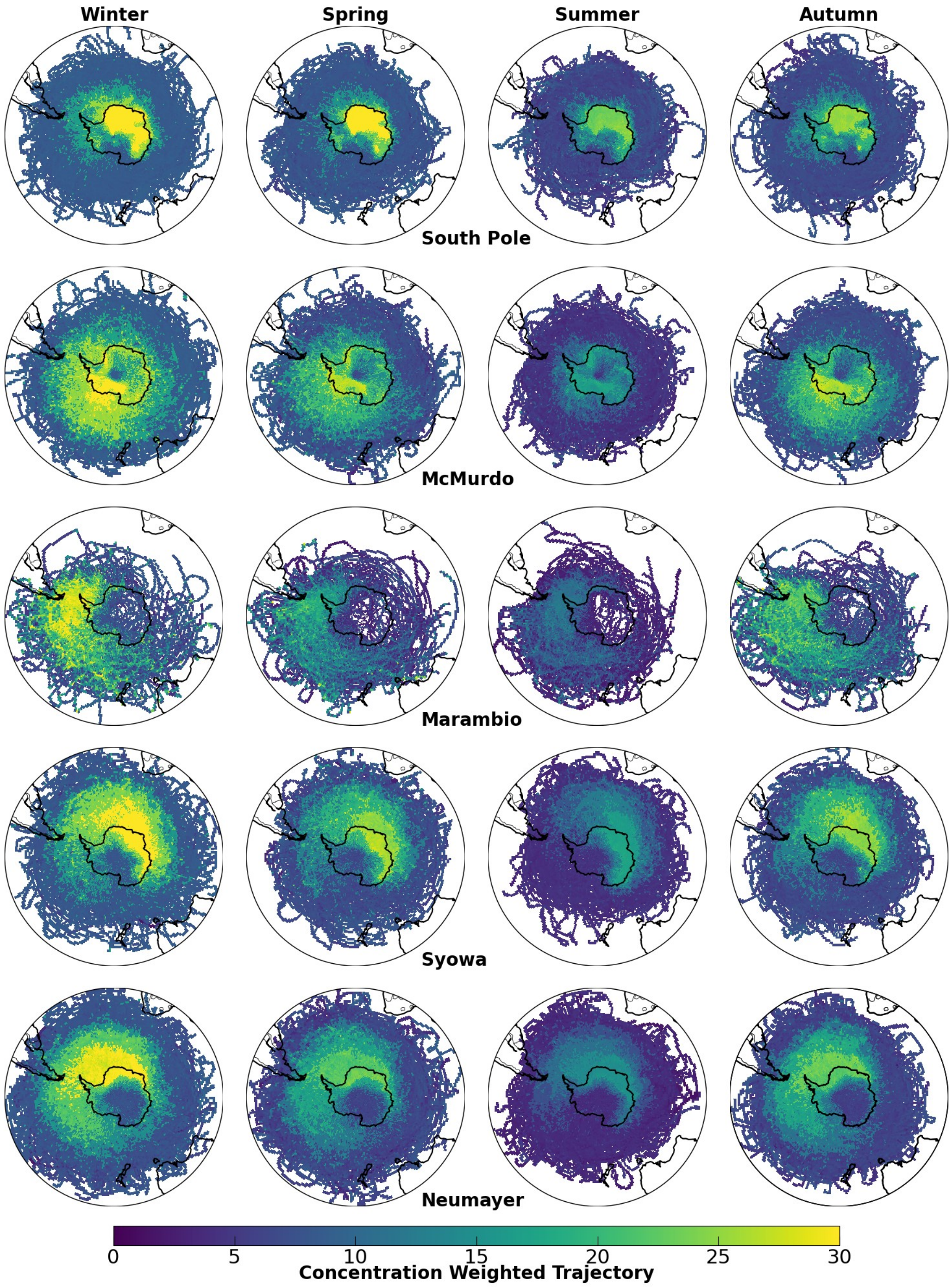

Figure S4: *Concentrated weighted trajectory (CWT) for surface ozone based on 15 days backward trajectories calculated using HYSPLIT at 500 meters above the ground level at various Antarctic based stations.*

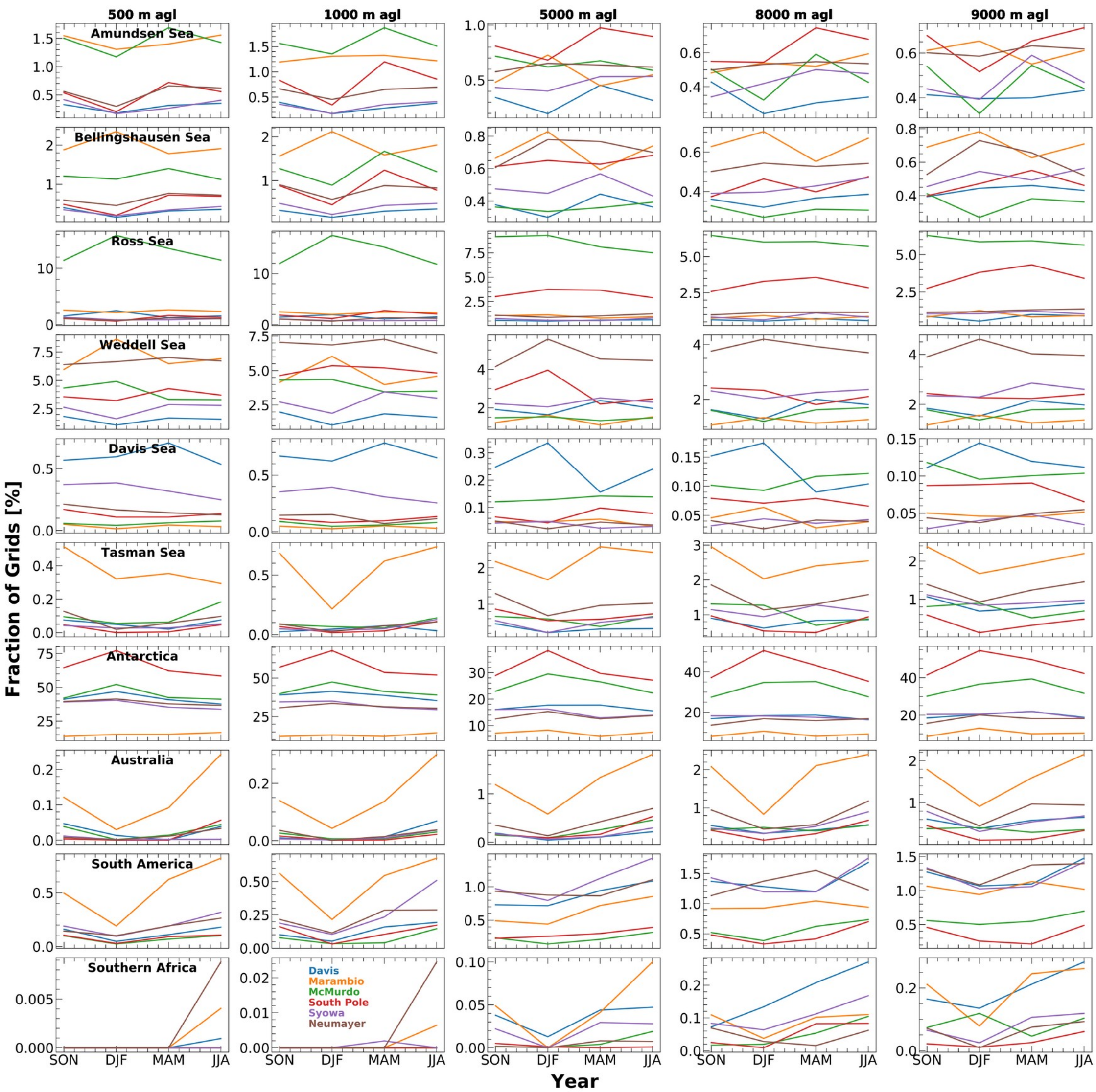

Figure S5: *Seasonal climatology of the contributions of various continents and Seas around the Antarctica (including Antarctica) to air mass transport at various stations at different altitudes above the ground level (agl).*

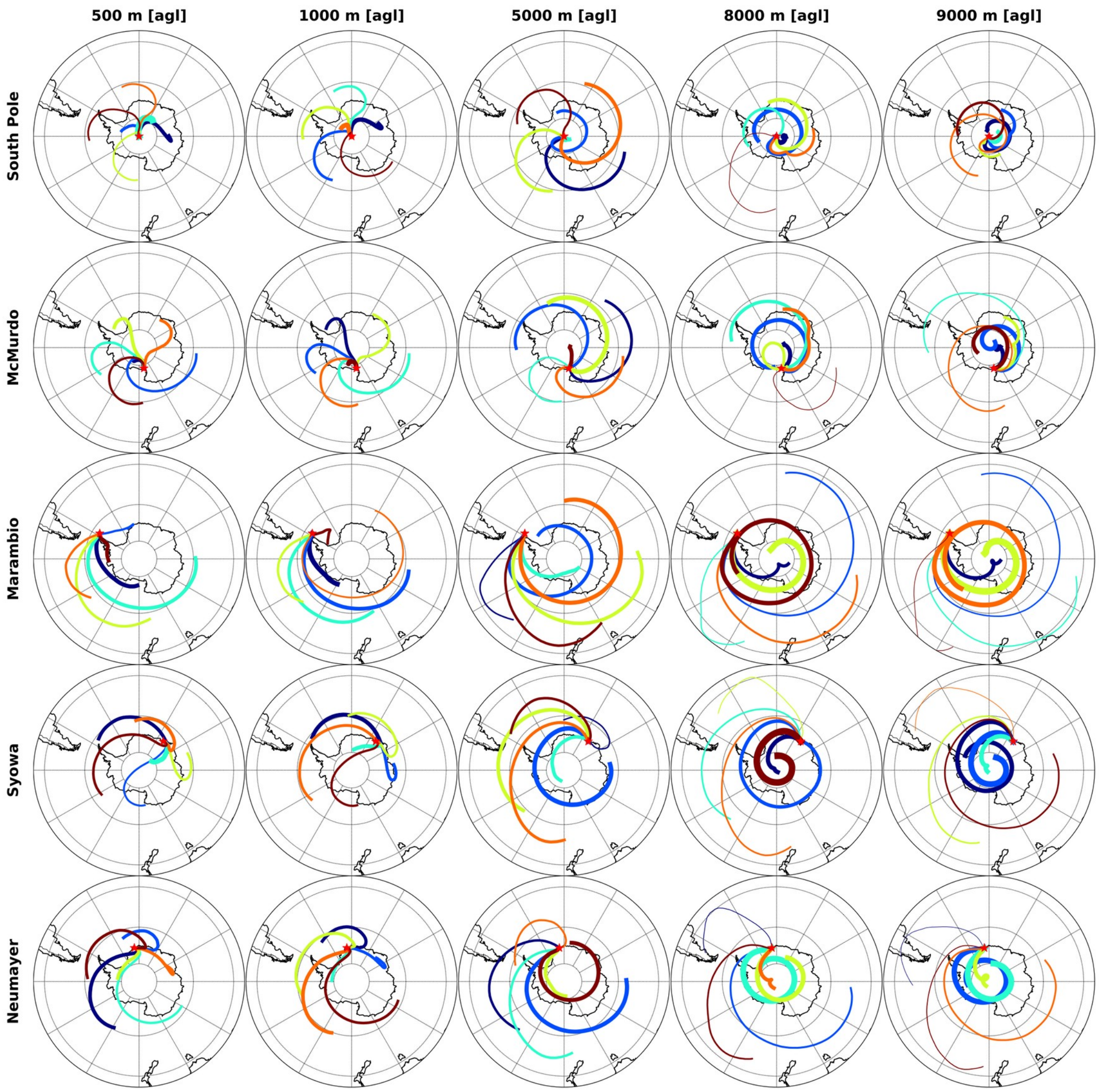

Figure S6: *Cluster of 15 days backward trajectories at different stations generated using HYSPLIT.*

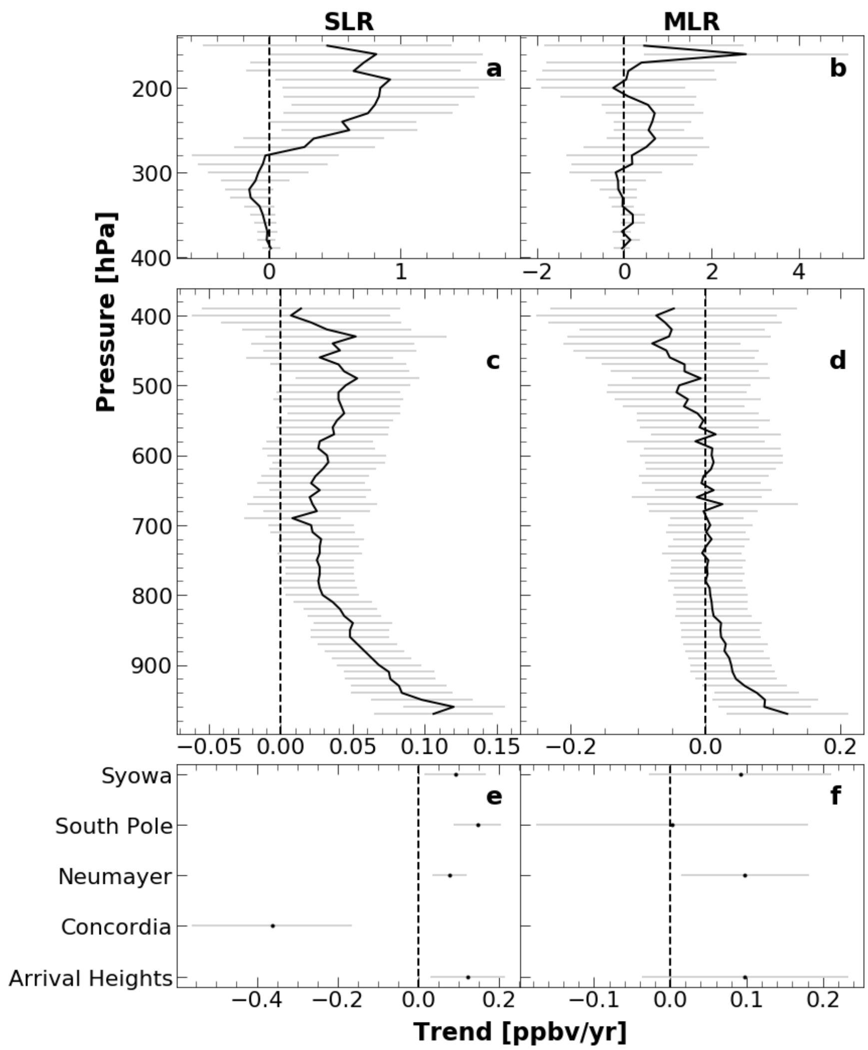

Figure S7: *Trends of annual ozone data estimated using SLR and MLR. (a–d) solid black line shows the mean trend and gray error-bars show 95% confidence interval of estimated trends at different pressure levels. (e–f) black dots show the mean surface ozone trend at various stations and gray error-bars show 95% confidence interval of estimated trends.*

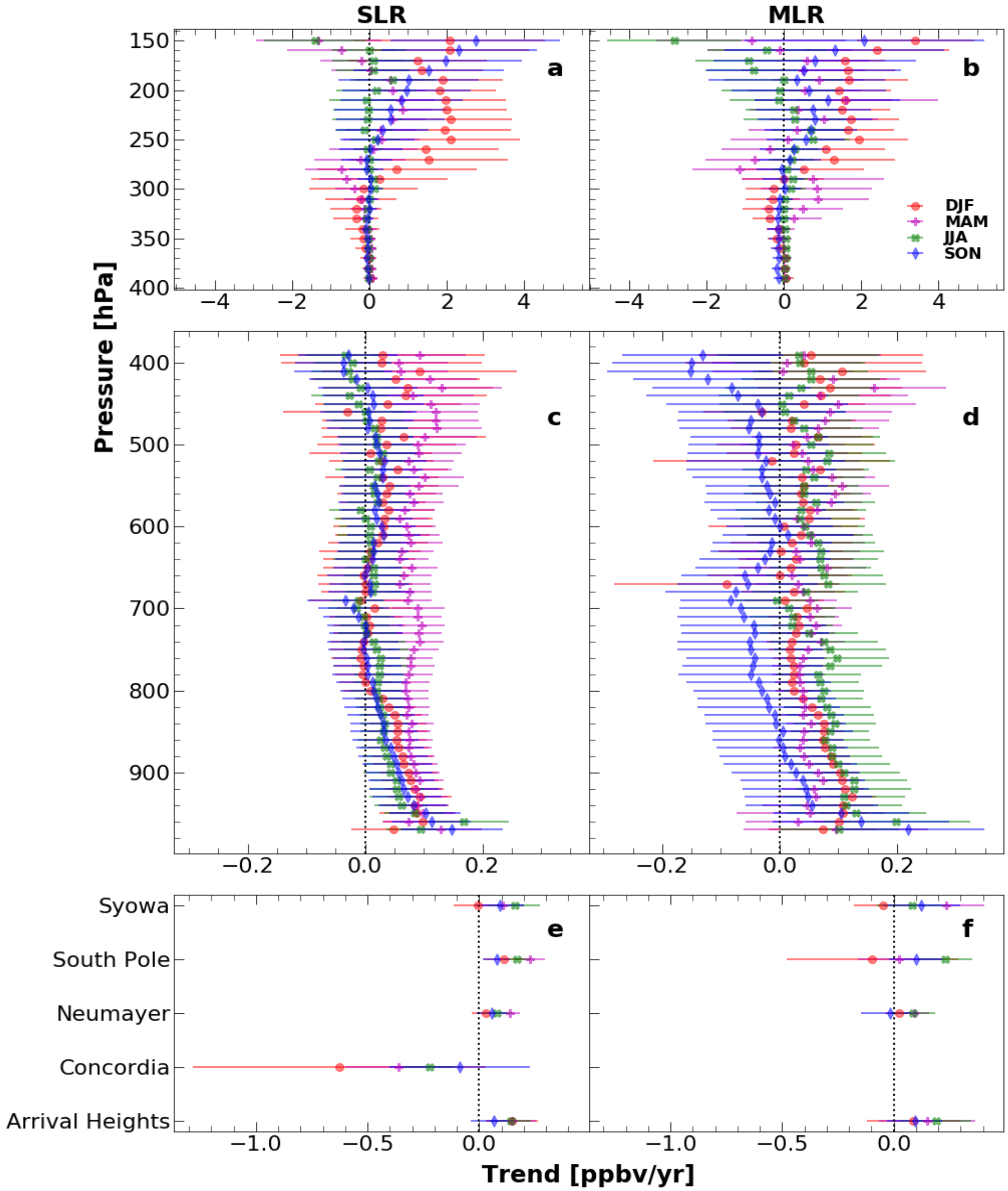

Figure S8: *Trends of seasonal ozone data estimated using SLR and MLR. (a–d) colored solid markers show the mean trend and error-bars show 95% confidence interval of estimated trends at different pressure levels. (e–f) colored solid markers show the mean trend and error-bars show 95% confidence interval of estimated trends.*

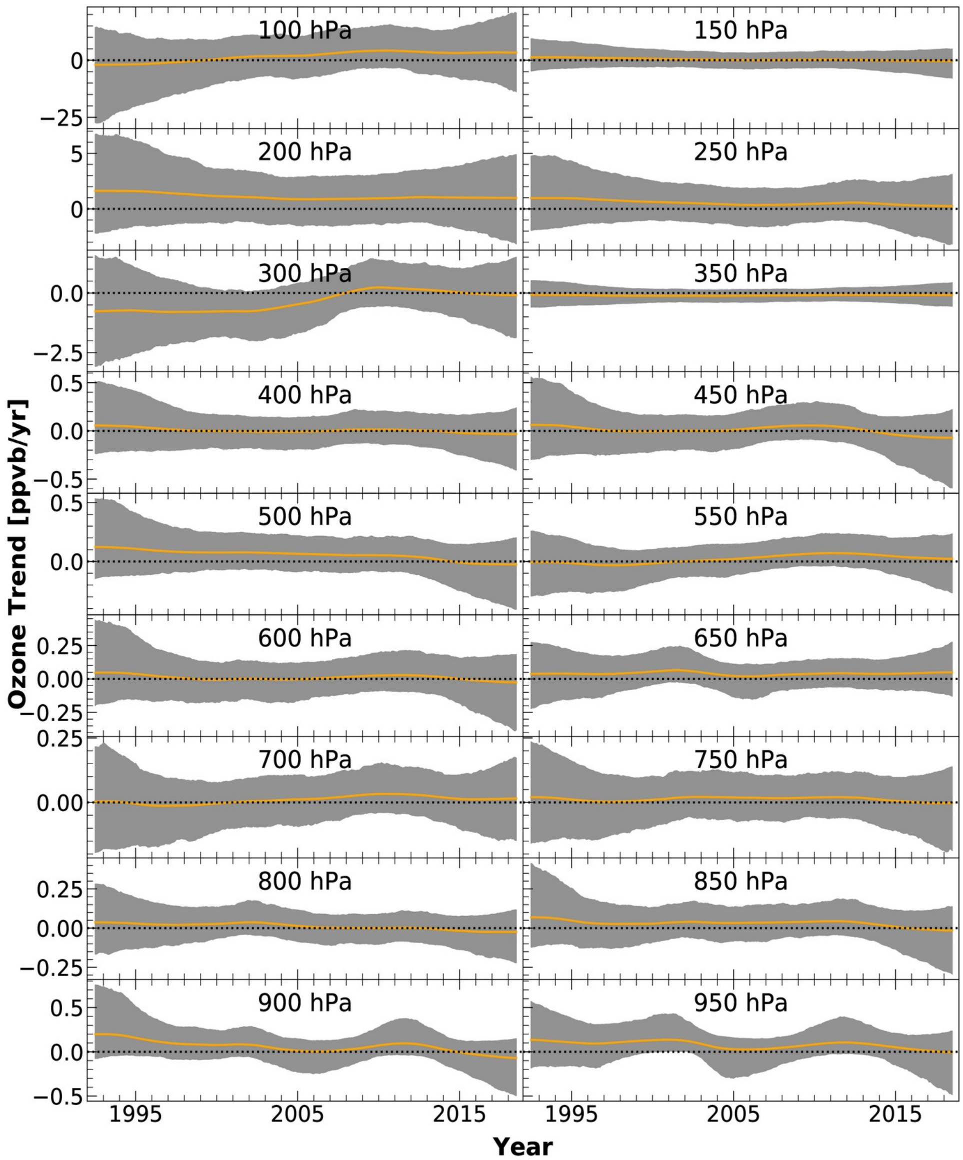

Figure S9: *Trends of monthly ozone data estimated using DLM at various vertical pressure levels. Here error-bars show 95% credible interval of estimated trends.*

Fig. S9 depicts the DLM trends and their variability for tropospheric ozone from 950 hPa till 100 hPa at 50 hPa intervals. Positive trend in lower troposphere is clear visible in the figure (from 950 hPa till 600 hPa). However, the trends seem to have turned negative in recent years. This negative turn in lower tropospheric trends in recent years is not discernible from MLR analysis.

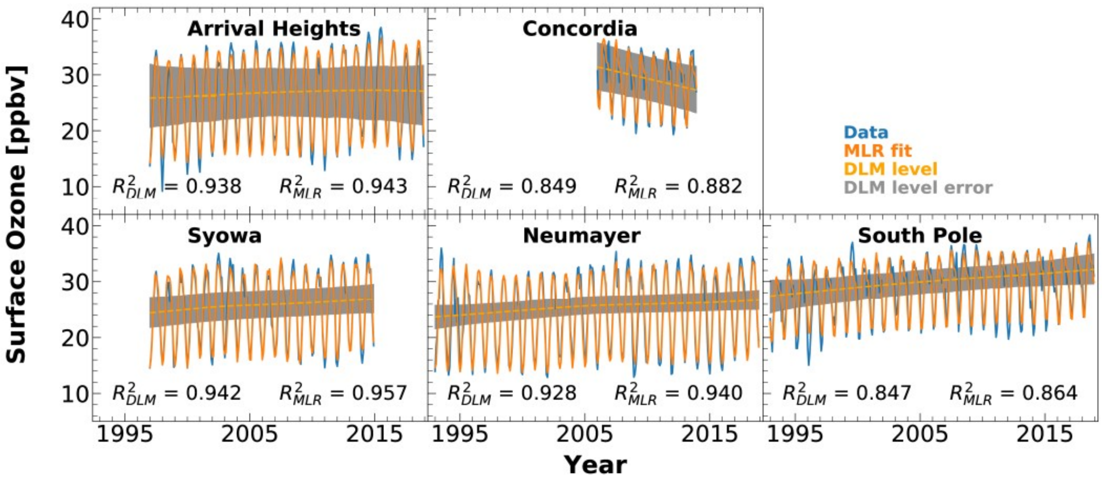

Figure S10: *Model fit (MLR and DLM) of surface ozone at various stations in Antarctica.*

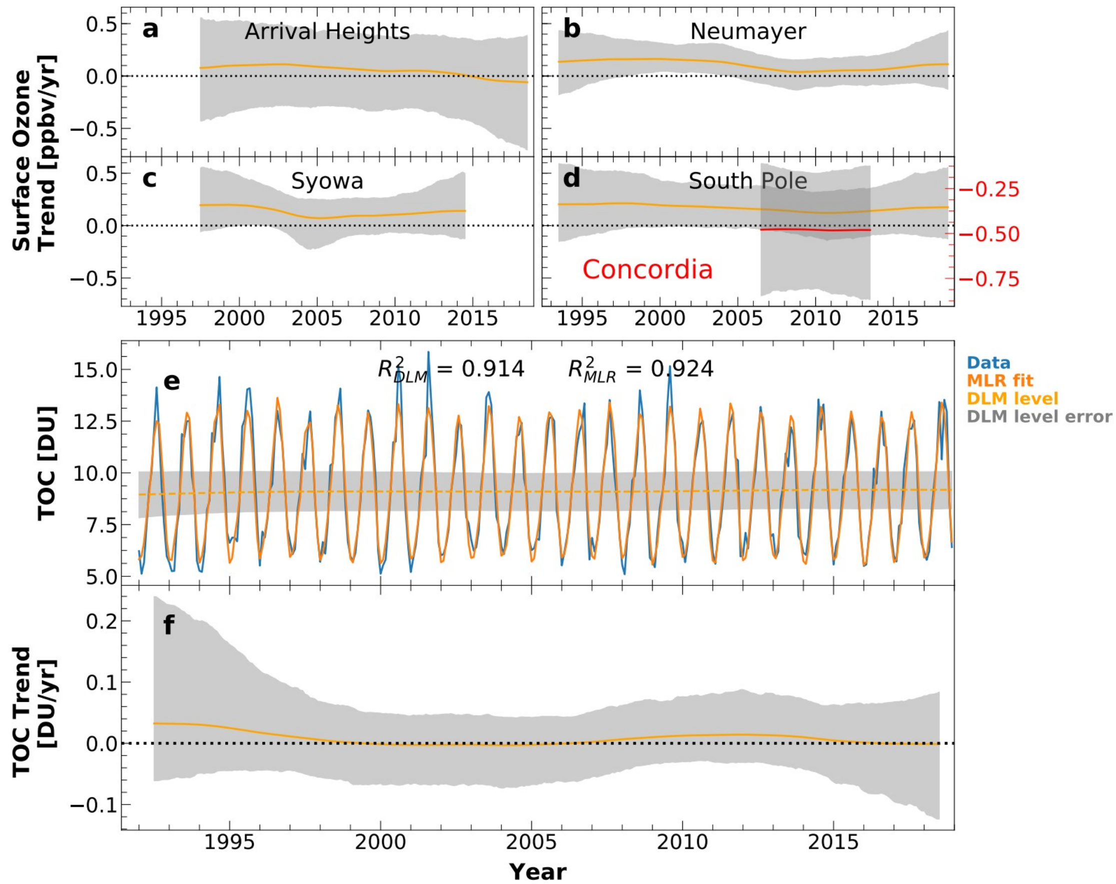

Figure S11: *(a–d) Bayesian dynamic linear model (DLM) trend of monthly mean surface ozone along with 95% credible interval at different stations. (e) Time-series of monthly mean tropospheric ozone column (TOC) with MLR fit and DLM background ozone (level) along with 95% confidence interval. (f) DLM trend of monthly mean TOC along with 95% credible interval.*

Fig. S11 depicts the DLM trends and their variability for surface ozone at various stations (a-d) and total ozone column (f). Surface ozone trends are positive throughout the study period for all stations except for Arrival Heights (after 2015) and Concordia. Similarly, TOC trends are also positive over the span of the study.

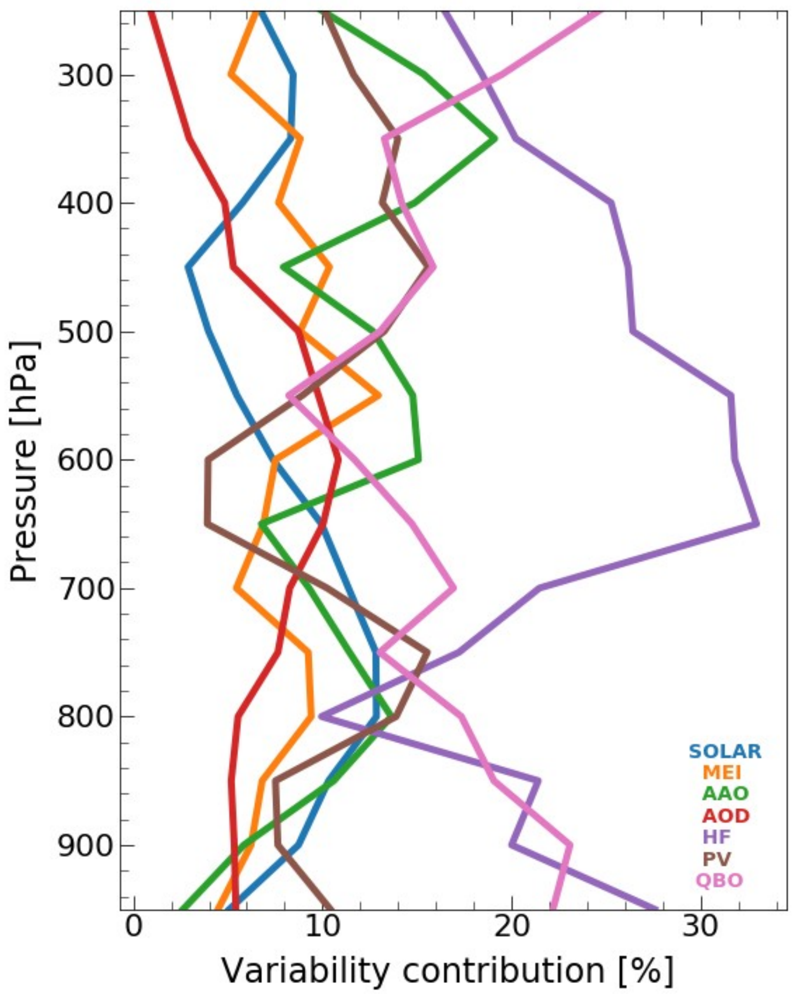

Figure S12: *Contribution of various proxies to inter-annual ozone variability at different vertical pressure levels.*

REFERENCES

(1) Laine, M.; Kyrölä, E.; Latva-Pukkila, N.; Kyrölä, E. Analysing time-varying trends in stratospheric ozone time series using the state space approach. *Atmospheric Chemistry and Physics* **2014**.

(2) Zanchettin, D.; Gaetan, C.; Arisido, M. W.; Modali, K.; Toniazzo, T.; Keenlyside, N.; Rubino, A. Structural decomposition of decadal climate prediction errors: A Bayesian approach. *Scientific Reports* **2017**, *7* (1), 12862.

(3) Ball, W. T.; Alsing, J.; Mortlock, D. J.; Rozanov, E. V.; Tummon, F.; Haigh, J. D. Reconciling differences in stratospheric ozone composites. *Atmospheric Chemistry and Physics* **2017**, *17* (20), 12269–12302.

(4) Ball, W. T.; Alsing, J.; Mortlock, D. J.; Staehelin, J.; Haigh, J. D.; Peter, T.; Tummon, F.; Stübi, R.; Stenke, A.; Anderson, J.; Bourassa, A.; Davis, S. M.; Degenstein, D.; Frith, S.; Froidevaux, L.; Roth, C.; Sofieva, V.; Wang, R.; Wild, J.; Yu, P.; Ziemke, J. R.; Rozanov, E. V. Evidence for a continuous decline in lower stratospheric ozone offsetting ozone layer recovery. *Atmospheric Chemistry and Physics* **2018**, *18* (2), 1379–1394.

(5) Alsing, J. dlmmc: Dynamical linear model regression for atmospheric time-series analysis. *Journal of Open Source Software* **2019**, *4* (37), 1157.